Food and Agricultural Immunology

ISSN: 0954-0105 (Print) 1465-3443 (Online) Journal homepage: https://www.tandfonline.com/loi/cfai20

Deciphering the binding mode of dinitramine herbicide to ct-DNA, a thermodynamic discussion

Mohammad-Ali Daneshmehr, Farhad Ahmadi, Bahare Ahmadi & Ebrahim Shakiba

To cite this article: Mohammad-Ali Daneshmehr, Farhad Ahmadi, Bahare Ahmadi & Ebrahim Shakiba (2016) Deciphering the binding mode of dinitramine herbicide to ct-DNA, a thermodynamic discussion, Food and Agricultural Immunology, 27:1, 23-39, DOI: 10.1080/09540105.2015.1055555

To link to this article: https://doi.org/10.1080/09540105.2015.1055555

Food and Agricultural Immunology, 2016
Vol. 27, No. 1, 23–39, http://dx.doi.org/10.1080/09540105.2015.1055555

Taylor & Francis
Taylor & Francis Group

Deciphering the binding mode of dinitramine herbicide to ct-DNA, a thermodynamic discussion

Mohammad-Ali Daneshmehr[a], Farhad Ahmadi[a,b]*, Bahare Ahmadi[c] and Ebrahim Shakiba[d]

[a]*Department of Medicinal Chemistry, Faculty of Pharmacy – International Campus, Iran University of Medical Sciences, Tehran, Iran;* [b]*Department of Medicinal Chemistry, Faculty of Pharmacy, Kermanshah University of Medical Sciences, Kermanshah, Iran;* [c]*Department of Toxicology (Pharmacy), Shahreza Branch Islamic Azad University, Isfahan, Iran;* [d]*Department of Clinical Biochemistry, Kermanshah University of Medical Sciences, Kermanshah, Iran*

(*Received 28 February 2015; accepted 22 May 2015*)

Dinitramine is a herbicide that has been used to control annual grasses and broadleaf weeds in cotton and soybeans in Iran. In this study, the electrochemical behavior of dinitramine was studied by cyclic voltammetry (CV) and differential pulse voltammetry (DPV) methods. The interaction of dinitramine with ct-DNA was evaluated by CV, competitive fluorescence, UV-Vis spectroscopy, FT-IR spectroscopy, and viscosity titration. In addition, the thermodynamic parameters of DIN–DNA complex were calculated by spectrophotometric titration. The values of $\Delta H_{bin.}$, $\Delta S_{bin.}$, and $\Delta G_{bin.}$ (T = 290.65 K) of the DIN–DNA complex were +39.25 kJ mol^{-1}, +215.71 J $mol^{-1,}$ and −23.45 KJ mol^{-1}, respectively. These data revealed that the endothermic binding has its origin in the hydrophobic interactions. Also the high positive ΔS_{bin} was explained according to the DIN structure that optimized by mechanical quantum calculations. However, all data showed that the major groove binding between DIN and ct-DNA is more predominant than other binding modes.

Keywords: dinitramine herbicide; DNA binding; major groove; thermodynamic parameters

1. Introduction

Today, the role of pesticides in our lives is fully felt (Stoytcheva, 2011). These compounds have two opposite effects: the first is increasing growth rate of human population via the enhancement of agricultural food productions, and the second is decreasing of human health quality. However, the vigorous development of various cancers may be due to the widespread use of pesticides (Frost, Brown, & Harding, 2011; Sathiakumar, MacLennan, Mandel, & Delzell, 2011). Therefore, pesticides have been considered as potential chemical mutagens (Liu, 2012). An important way to assess mutagenic and carcinogenic properties of these compounds is evaluate their ct-DNA binding abilities as a critical point to consider them as mutagen and also carcinogen materials. So, in recent years several in vitro studies focusing on effects of pesticides on DNA damage were carried out (Ahmadi, Alizadeh, Bakhshandeh-Saraskanrood, Jafari, & Khodadadian, 2010; Ahmadi & Bakhshandeh, 2009; Ahmadi & Ghanbari, 2014;

*Corresponding author. Email: fahmadi@kums.ac.ir

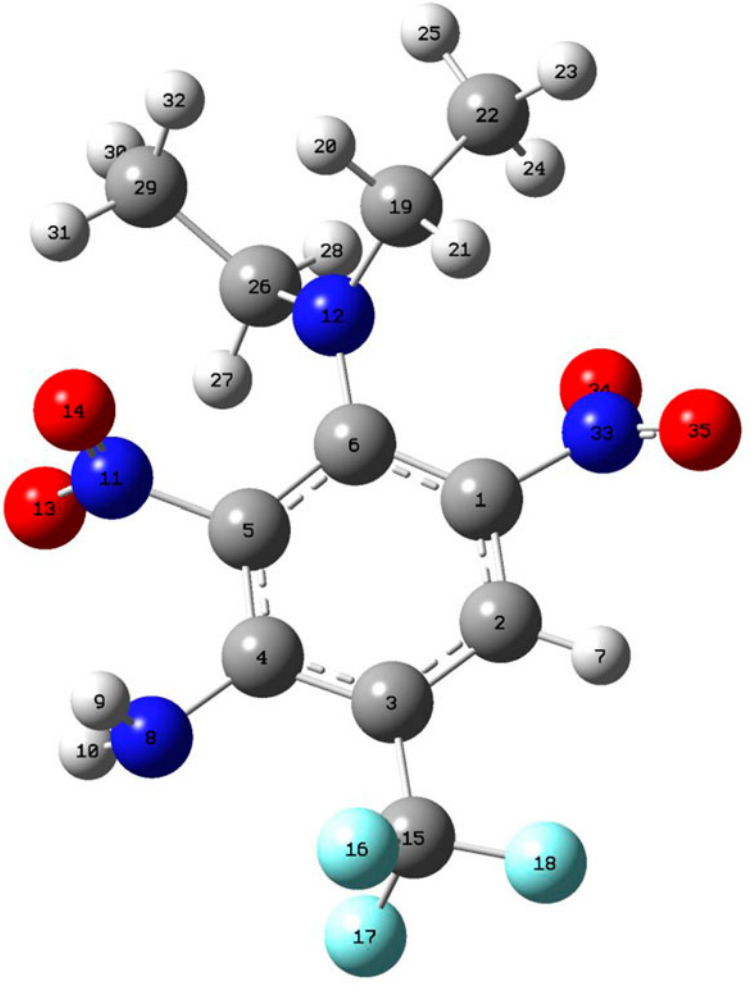

Figure 1. The optimized structure of dinitramine (DIN) that was measured by DFT at B3LYP, 6–31 G++(d, P).

Kashanian, Askari, et al., 2008; Kashanian, Gholivand, Ahmadi, & Ravan, 2008; Zhang, Hu, Zhao, Li, & He, 2010).

Dinitramine (N_3,N_3-diethy1-2,4-dinitro-6-trifluoromethyl-*m*-phenylenediamine [DIN]; Figure 1) is structurally related to substituted dinitroaniline herbicides and widely used for controlling annual grasses and broadleaf weeds in cotton and soybeans (Berg, 1974).

Earlier studies demonstrated that after 100 days the amount of DIN in soil was decreased by around 10% and this compound was strongly absorbed by soil (Smith, Belle, Shen, & Woods, 1973). It is well shown that the substituted dinitroaniline compounds have strong mutagenic and toxic effects (Thompson, Hill, Epp, & Probst, 1983). Olson et al. demonstrated that DIN is toxic to fish and accumulates in fish tissue after brief exposures to low concentrations (Olson, Allen, Mauck, & Agric, 1975). El-Khadem et al. demonstrated that DIN has a remarkable effect on the development of Rhizoctonia disease in cotton and has highly phytotoxic effect (El-Khadem, Zahran, &

El-Kazzaz, 1979). However, according to our library search a little information existed about the DIN, therefore, in this study the electrochemical behavior of DIN was studied. In addition, the interaction of DIN with ct-DNA and the structural changes of ct-DNA were investigated in 10 mM Tris-HCl buffer at neutral pH = 7.3, using viscosity titration, voltammetric and spectroscopic (UV-Vis, FT-IR, and fluorescence) procedures. Also, the thermodynamic parameters of DIN–DNA complexation were measured and the mode of binding was discussed.

2. Experimental section

2.1. Materials and reagents

The highly polymerized calf thymus DNA (ct-DNA) was purchased from Sigma Chemical Co. (USA). The high purity (99.5%) of dinitramine was purchased from Fluka. The MeOH, Tris, HCl, AgCl, and Ethidium bromide (EB) were analytical grade and purchased from Merck (Darmstadt Germany). Double distilled and deionized water was used throughout the study. The stock solution of ct-DNA was prepared according to our previous study as follows: the stock solution of ct-DNA was prepared by dissolving ct-DNA in Tris–HCl buffer (pH 7.3) and dialyzing exhaustively against the same buffers for 24 h. A solution of ct-DNA gave a ratio of UV absorbance at 260 and 280 nm more than 1.8, indicating that ct-DNA was sufficiently free from protein (Ahmadi, Ebrahimi-Dishabi, Mansouri, & Salimi, 2014).

2.2. Apparatus

An HP Agilent (8453) UV-Vis spectrophotometer equipped with a Peltier (Agilent 89090A) was used for studying spectrophotometric titrations. All competitive fluorescence measurements were carried out with a Beckman spectrofluorometer (LS 45). Maximum excitation wavelength of DNA–EB complex used was 497 nm. The viscometric titrations were performed by a Schott Gerate AVS 450 automated viscometer at 298 ± 0.05 K. The time of the solution's flowing through the capillary was determined by a stopwatch. The pH values of solutions were measured by a Metrohm pH meter model 827.

The cyclic voltammetric (CV) and differential pulse voltammetric (DPV) measurements were carried out by a voltammeter VA 797 Computrace (Metrohm) at a hanging mercury drop electrode (HMDE). An Ag/AgCl as reference electrode (3 mol L^{-1} KCl) and a platinum wire as an auxiliary electrode were used. For all types of voltammetric measurements, the supporting electrolyte (0.01 mol L^{-1} Tris-HCl buffer solution, pH = 7.3) was placed in a voltammetric cell of volume 10 mL and deaerated via purging with pure N_2 gas for 2.0 min. The CV measurements were carried out by keeping both concentrations of the DIN and the total volume of solution constant, while, the ct-DNA concentrations varied. The FT-IR measurement was carried out by using Shimadzu (IR Prestige-21) equipped with a KBr beam splitter.

2.3. CV titrations of DIN with ct-DNA

The CV titrations were carried out by keeping both concentration of the DIN (5.0×10^{-5} mol L^{-1}) and total volume of solution constant, while the ct-DNA concentration varied (0.0–5.0×10^{-4} mol L^{-1}; R_i = [DNA]/[DIN] = 10). Subsequently, a single-sweep CV

experiment was performed at a given scan rate 90 mV s^{-1}, with an initial potential of 0.0 V and a vertex potential of −1.0 V.

2.4. DPV titrations of DIN with ct-DNA

The cathodic DPV titrations were carried out at a constant concentration of the DIN (5.0×10^{-5} mol L^{-1}) and various concentrations of ct-DNA which caused the r_i = [DNA]/[DIN] = 0.0, 0.1, 0.3, 0.5, 0.7, and 1.0. The DP voltammograms were recorded in the initial potential of −0.3 V to end potential of −1.0 V.

2.5. Spectrophotometric titration of DIN with ct-DNA

The spectrophotometric titrations of ct-DNA with DIN were carried out as follow: 1.0 µl of DIN (1.0×10^{-2} mol L^{-1}) was added into a quartz cell containing 2.0 ml solution of ct-DNA (5.0×10^{-5} mol L^{-1}) by a Hamiltonian micro-syringe and the spectrum of solution was recorded at a constant temperature. The addition of DIN into the solution continued until the desired r_i = [DIN]/[DNA] = 1.0 was achieved. At this given r_i no spectrum change was observed. The binding constant (K_b) was measured using the following calculations:

$$\mathrm{DIN} + \mathrm{DNA} \leftrightarrow \mathrm{DIN} - \mathrm{DNAcomplex} \tag{1}$$

$$K = \frac{[DIN - DNAcomplex]}{[DNA]_{\mathrm{uncomplexed}}[DIN]_{\mathrm{uncomplexed}}} \tag{2}$$

For weak binding affinities, the data were treated using linear reciprocal plots based on the Equation (3) (Ahmadi, Jamali, Moradian, & Astinchap, 2012):

$$\frac{1}{A - A_0} = \frac{1}{A_\infty - A_0} + \frac{1}{K_b(A_\infty - A_0)} \cdot \frac{1}{[DIN]} \tag{3}$$

Where, A_0 is the absorbance of ct-DNA at 260 nm in the absence of DIN, A_∞ is the final absorbance of the DIN–DNA, and A is the recorded absorbance at different DIN concentrations. The plot of $1/(A - A_0)$ versus 1/[DIN] is linear and the binding constant (K_b) can be calculated from the ratio of the intercept to the slope (Ahmadi et al., 2012).

2.6. Competitive fluorescence study of interaction of DIN with EB-DNA complex

The competitive fluorescence investigations were performed by adding small aliquots of DIN stock solution (2 µl, 0.01 mol L^{-1}) into the 2 ml solution of DNA–EB (5.0×10^{-5} mol L^{-1} ct-DNA) complex. The excitation wavelength was 497 nm and the emission wavelength was 598 nm and the changes of fluorescence intensity were recorded.

2.7. Viscosity experiments

For viscosity titrations the concentration of ct-DNA was 5.0×10^{-4} mol L^{-1} and three measurements were tested to calculate the average relative viscosity η of the ct-DNA solution in presence of increasing amounts of DIN. The data were reported as ($\eta/\eta\circ$) versus the r_i (r_i = [DIN]/[DNA]), where $\eta\circ$ is the viscosity of the ct-DNA solution alone.

2.8. FT-IR studies for interaction of ct-DNA with DIN

The FT-IR spectra of the DIN–DNA complex were recorded on the AgCl cell. The spectra of two solutions of DIN–DNA complex with R_i = [DNA]/[DIN] = 40, 4 (DNA = 5.0×10^{-3} mol L^{-1}) were recorded in the spectral range of 2000–500 cm^{-1} with a nominal resolution of 2 cm^{-1} and a maximum of 20 scans. The blank windows and water were removed by BGK mode of instrument according to our previous study (Ahmadi, Jafari, et al., 2013). The spectra smoothed with Golly procedure.

2.9. The computational optimization of DIN

The geometric optimization of DIN was carried out by the conventional DFT method in aqueous medium by using of DFT theory at B3LYP (Miehlich, Savin, & Preuss, 1989) level. Pople type 6-31++G (d,p) (Petersson & Al-Laham, 1991) was employed for our calculations. Polarization functions (Roux & Simonson, 1999) are added to give additional flexibility for the description of molecular orbital. However, the polarization and diffuse functions are the correction functions, which describe the deformation and diffuse of the electronic cloud. The water effect was evaluated with utilization of the polarized continuum model (PCM), initially proposed by Miertus, Scrocco, and Tomasi (1981). In this method, the solute cavity may be specified as a set of overlapping spheres, thus allowing for a more realistic cavity shape for extended molecules, in contrast to other solvation models (Colominas, Luque, & Teixido, 1999).

3. Results and discussions

3.1. The UV-Vis titration and thermodynamic measurements

The spectrophotometric titration of ct-DNA by DIN with r_i = [DIN]/[DNA] = 0.0, 0.1, 0.2, 0.3, 0.4, 0.5, 0.6, 0.7, 0.8, 0.9, 1.0 at four different temperatures (10, 15, 20, and 25° C) were measured, and the UV-Vis spectrum of 10°C is shown in S1a.

DNA has an absorption peak at 260 nm, due to the $\pi-\pi^*$ transitions of nucleotides. By adding more DIN into the DNA solution a remarkable hyperchromic and red shift (~5 nm) at peak 260 nm was observed. The increase of the absorbance is due to the changes in ct-DNA structure when DIN was added to ct-DNA solution. The same hyperchromic shifts have already been reported for ct-DNA interaction with 2,4-D, pyriproxyfen and fenitrothion (Ahmadi & Bakhshandeh, 2009; Ahmadi & Jafari, 2011; Ahmadi et al., 2012). This increase of ct-DNA spectrum along with red shift (hyperchromic and bathochromic effects) is due to the interaction of DIN with base pairs of ct-DNA and changes of ct-DNA double helixes. As it is observed from S1a, the peak position of ct-DNA moved toward higher wavelengths and we believed that the DIN may induce a change in the helical conformation of ct-DNA structure and open it via grooves binding interactions. The binding equilibrium constant of DIN–DNA complex was calculated as described in Section 2.4. S1b represents the plots of $1/(A - A_0)$ versus 1/[DIN] in four different temperatures (283, 288, 293, 298 K); the binding constant (K_b) was calculated from the ratio of the intercept to the slope. By comparison of obtained K_b value at 25°C of DIN–DNA ($K_b = 2.310^4$) with ethedium bromid-DNA complex (1.4×10^6 in 40 mM NaCl + 25mM Tris–HCl) (Waring, 1965), it is concluded that the mode of binding is not intercalation. Several studies have reported the K_b of ct-DNA with various pesticides which were obtained by spectrophotometric titration such as: fenitrithion (1.9×10^4) (Ahmadi & Jafari, 2011), 2-imidazolidinethione (1.4×10^3) (Ahmadi et al., 2010), 2,4-D

(3.5×10^3 and 5.0×10^3) (Ahmadi & Bakhshandeh, 2009), clodinafop-propargyl (5.6×10^3) (Kashanian, Askari, et al., 2008), diazinon (1.6×10^4) (Kashanian, Gholovand, et al., 2008), pyriproxyfen (2.8×10^4) (Ahmadi et al., 2012), and aminocarb (7.2×10^3) (Zhang et al., 2010). However, our data show that the DIN–DNA has an affinity similar to the non-intercalators. As the structure of ct-DNA was changed by DIN, the thermodynamic stability of ct-DNA was changed too. So, the evaluation of thermodynamic parameters of binding i.e., $\Delta H_{bin.}$, $\Delta S_{bin.}$, and $\Delta G_{bin.}$ may be helpful for elucidating the mode of interaction. The thermodynamic parameters were calculated using van't Hoff equation ($K_b = e^{-\Delta G/RT}$) via plot *log* K_b versus $1/T$ (see S1c). The negative slope in the van't Hoff plot indicates that the complexation process is endothermic. The $\Delta H_{bin.}$, $\Delta S_{bin.}$, and ΔG_{bin} (T = 290.65 K) values of the DIN–DNA complex were +39.25 kJ mol^{-1}, +215.71 J $mol^{-1,}$ and −23.45 KJ mol^{-1}, respectively. Based on thermodynamic data the complex formation was enthalpy disfavored and entropy favored. The structure of DIN in water medium was optimized by GAUSSIAN 03 (Frisch et al., 2003) package using the density functional theory (DFT; Becke, 1993) as described in Section 2.9. Some geometrical parameters such as bond lengths and dihedral angles which were computed with the above method are presented in Table 1.

DIN molecule has a planar geometry as predicted by ab initio quantum chemical method used here as shown from the dihedral angles in Table 1. In addition, the calculated natural atomic charges of DIN are listed in Table 1, too. As data of Table 1 show, it is concluded that the DIN exhibited charge delocalization, except in C15 of –CF3 moiety. In addition, the dipole moment of DIN was 1.4642 Debye. The dipole moment which is the first derivative of the energy with respect to an applied electric field is a measure of the asymmetry in the molecular charge distribution. The low values of the dipole moment suggest that the hydrophobic interaction of DIN molecule plays another role in the interaction with nucleobases. The same result was already reported for interaction of psoralen and 8-methoxy psoralen with nucleobases (El-Gogary & Koehler, 2007). According to mechanical quantum the DIN has a weak dipole moment and therefore the water molecules were easily released during interaction with ct-DNA and caused high positive $\Delta S_{bin.}$. Hans and Becker in a study demonstrated when a small molecule was transferred from a polar to a nonpolar environment; hydrophobic interaction caused $\Delta H > 0$ and $\Delta S > 0$ accompanied by a negative ΔG (Hans, Becker, & Am, 1997). In other words, the positive entropy change is frequently regarded as evidence for a hydrophobic interaction, because water molecules that are arranged in an orderly fashion around the DIN and ct-DNA were released and the positive $\Delta H_{bin.}$ value observed may be attributed to the non-intercalation binding.

3.2. The competitive fluorescence titration study

The EB caused a dramatic enhancement of ct-DNA fluorescence efficiency when intercalated into ct-DNA. If an analyte molecule intercalated into the double strand of ct-DNA, the fluorescence of EB-DNA complex is quenched via competition between EB and analyte molecule for binding sites in ct-DNA (Ahmadi, Jamali, et al., 2011). Therefore, in order to prove intercalation mode of DIN–DNA interaction, the quenching of EB fluorescence was studied. Figure 2 shows the fluorescence spectrum of EB-DNA in absence and presence of different amounts of DIN.

As it is observed, by adding the DIN no quenching of EB-DNA fluorescence was observed. Ling et al. in a study conducted on the interaction of pazofloxacin with ct-DNA

Table 1. Selected geometrical parameters and natural charges calculated with density functional method using B3LYP-6.31G++(d,p) for DIN molecule.

DFT-B3LYP-6.31G++(d,p)-CPCM in water medium					
Atoms	Bound length (A) Dihedral Angels (degree)	Atoms	Natural charge	Atoms	Natural charge
C1-N33	1.47 A	C1	−0.315	N33	−0.444
C5-N11	1.48 A	C2	−0.424	N8	−0.566
C4-N8	1.42 A	C3	0.016	N11	−0.460
C6-N12	1.38 A	C4	−0.730	N12	0.277
C19-N12	1.47 A	C5	−0.186	O13	0.089
C26-N12	1.47 A	C6	−0.742	O14	0.078
N8-C4-C5-C3	−177.65	C15	2.041	O34	0.081
N33-C1-C6-C2	−177.14	C19	0.317	O35	0.078
C15-C3-C2-C4	179.37	C22	−0.584	F16	−0.258
C22-C19-N12-C5	129.17	C26	0.342	F17	−0.259
C29-C26-N12-C5	122.80	C29	−0.561	F18	−0.338

by competitive fluorescence believed that the compound interacts with ct-DNA by intercalation if the emission intensity of the DNA–EB system decreases more than 50% and if the ratio of the concentration of drug to DNA is less than 100 (Ling, Zhong, Huang, & Ni, 2003). The intensity of DNA–EB system was not changed and this indicates that DIN binds to ct-DNA in a different mode from EB.

3.3. FT-IR interaction study of DIN to ct-DNA

The FT-IR was used as another evidence for determining the structural variations of the ct-DNA, and sequence preference. The FT-IR spectra of ct-DNA and DIN–DNA with r_i = [DIN]/[DNA] = 1/40 and 1/4 are presented in Figure 3a–c.

Figure 3a represents the FT-IR spectrum of free ct-DNA. The vibrational bands of ct-DNA at 1703.4, 1651.0, 1606.5, and 1489.0 cm^{-1} are assigned to guanine (G), thymine (T), adenine (A), and cytosine (C) nitrogenous bases, respectively. Additionally, the bands at 1232.5 and 1091.7 cm^{-1} are assigned to phosphate asymmetric and symmetric vibrations, respectively. The band at 1058.9 cm^{-1} is assigned to the sugar vibration.

By adding DIN into the solution with r_i = 1/40, the bands of 1703.4, 1651.0, 1606.5, and 1489.0 cm^{-1} were shifted to the 1705.0, 1645.2, 1608.7, and 1487.1 cm^{-1} (Figure 3b). All peaks were reduced by 7–19%. In addition, the bands of 1232.5, 1091.7, and 1058.9 cm^{-1} were not shifted and remained constant and confirmed no outside binding and or backbone binding were occurred. These vibrations shifts of all bands of nucleotide bases decreased intensity of all these bands vibrations and can be attributed to a change conformation of ct-DNA due to interaction of DIN with ct-DNA grooves. As DIN concentration increased (r_i = 1/4), the peaks of 1703.4, 1651.0, 1606.5, and 1489.0 cm^{-1} were shifted to the 1701.2, 1656.8, 1606.7, and 1477.4 cm^{-1} (Figure 3c). In addition, the peaks of 1232.5 and 1058.9 cm^{-1} were shifted to the 1236.3 and 1062.7 cm^{-1}. The peaks of guanine and cytosine significantly reduced more than those of adenine and thymine. The vanish of cytosine band and higher decrease in the guanine band than the other base pairs (A-T) and phosphate and sugar bands show that the DIN has more interaction with the G-C base pairs. A major

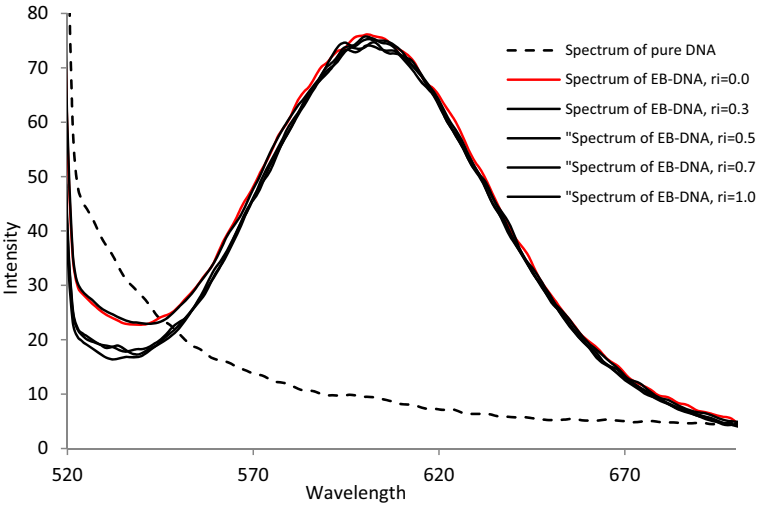

Figure 2. Emission spectrum of EB-DNA complex (5.0×10^{-5} mol L^{-1} of DNA) in the Tris-HCl buffer (Red line) in presence different amounts of DIN (r_i = 0.0, 0.1, 0.3, 0.5, 0.7, and 1.0).

decrease in the intensities of cytosine band was observed. However, these results indicate that the interaction of DIN with ct-DNA occurred more via major groove than the minor groove and/or backbone phosphate (N'soukpoe-Kossi et al., 2008).

3.4. Determination of viscosity

For further exploration of the intercalation and/or groove binding modes of DIN into the ct-DNA, the hydrodynamic method such as viscosity measurements was carried out on ct-DNA solution by varying the concentration of the added DIN. The values of relative specific viscosity ($\eta/\eta\circ$) versus r_i (r_i = [DIN]/[DNA]) in the absence and presence of DIN are shown in S2.

When an intercalation process occurs the double strand of ct-DNA becomes unwinding, lengthening, and causes the viscosity of the solution to increase. In other words, when a molecule is inserted between the ct-DNA base pairs, it leads to separation of base pairs and therefore, causes an increase in overall ct-DNA contour length. While, in groove binding mode a few effects on viscosity of solution are observed (Wilson, Barton, Tanious, Kong, & Strekowski, 1990). As it is observed from S2 the viscosity of ct-DNA solution is increased very little by adding DIN. This small interesting increase in viscosity suggests that the hydrogen interaction of the DIN with ct-DNA surface encouraged by the stronger hydrophobic bonding interactions in major groove, leads to un-bending (non-kinking) of the ct-DNA chain.

3.5. Electrochemical behavior of DIN and interaction with DNA

DIN is a derivative of dinitroaniline compounds and has two $-NO_2$ moieties that can be reduced at HMDE. The CV behavior of 5.0×10^{-5} mol L^{-1} of DIN at HMDE in scan rates of 10, 20, 30, 40, 50, 60, 70, 80, 90, 100, 120, 160, and 200 mV s^{-1} was studied in absence and presence of ct-DNA (see Figure 4a).

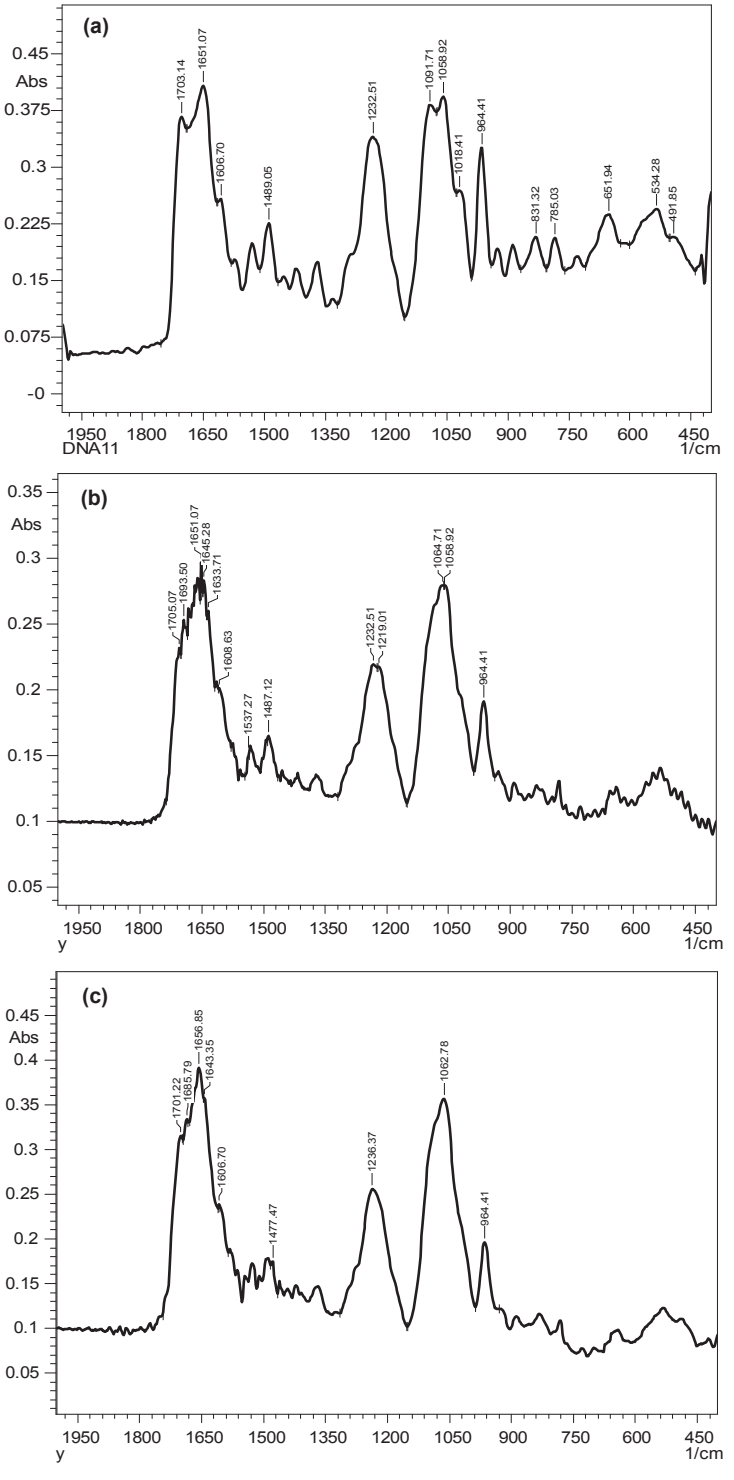

Figure 3. FT-IR spectrum in the region of 2000–500 cm^{-1} for (a) pure ct-DNA (0.005 mol L^{-1}), (b) in presence of DIN with r_i = [DIN]/[DNA]=1/40, and (c) r_i = [DIN]/[DNA] = 1/4.

As it is observed, in neutral media (pH = 7.3) and at HMDE two irreversible cathodic peaks at −0.44 V (scan rate 50 mVs^{-1}, peak I) and −0.571 V (scan rate 50 mVs^{-1}, peak II) were obtained. In our previous study we showed that in pH = 7.3 the $–NO_2$ moiety of molecules can be easily reduced to –NHOH by 2e and $2H^+$ mechanism at HMDE (Ahmadi & Jamali, 2012). Therefore, we concluded that the cathodic peaks I and II may correspond to the reduction of the nitro groups of $–NO_2$ at the electrode surface. To measure all electrons and symmetry of the energy barrier of cathodic peaks I and II, the Equation (4) was used (Ahmadi & Ghanbari, 2014).

$$\left|E_p - E_{p/2}\right| = 1.857\frac{RT}{\alpha nF}(mV) \tag{4}$$

Where $E_{p/2}$ is the potential, where $i = i_{p/2}$ in cyclic voltammograms. For exact measurement of $\left|E_p - E_{p/2}\right|$ all CV peaks were obtained by using the determination mode of the Metrohm VA 797 computrace instrument (Ahmadi & Ghanbari, 2014). The values of $\left|E_p - E_{p/2}\right|$ for cathodic peaks I and II at scan rate of 50 mV s^{-1} and 25°C were calculated as 36.6 and 41.66 mV, respectively. The values of $(\alpha n)_{\mathrm{I}}$ and $(\alpha n)_{\mathrm{II}}$, were measured as 1.30 and 1.14, respectively**.** If we assume that for an irreversible electrode process α value is equal to 0.5, therefore, the peaks I and II were reduced by two electrons. Additionally the real values of α for peaks I and II were 0.65 and 0.57, respectively.

Also, the values of αn of peaks I and II were measured from the slope of E_{pc} versus log υ (curve was not shown). For T = 298, and R = 8.314 and F = 96480 the slopes for peaks I and II were 0.046 and 0.05, respectively, therefore, the αn was obtained as 1.28 and 1.34, respectively. The α can be calculated by Bard and Faulkner (2004) as follows:

$$\alpha = \frac{47.7}{E_p - E_{p/2}} \tag{5}$$

The values of α for peaks I and II obtained were 0.64 and 0.59, respectively. Therefore, the number of electrons (n) transferred in the peaks I and II was calculated as 2 and 2.27≈2, respectively.

The dependence of the reduction peak currents of DIN on scan rate in the absence and presence of ct-DNA was studied and results are shown in Figure 4b. As it is observed, by increasing the scan rate, all cathodic peaks of DIN in absence of ct-DNA were nonlinearly increased.

Also, the peak potentials (E_{pc}) of peaks I and II shifted to more negative values with increasing the scan rate (see S1). These shifts proved that the electrochemical behavior of DIN is an irreversible process (Ahmadi & Jafari, 2011). The plots of i_p versus $\upsilon^{1/2}$ of all peaks in absence and presence of ct-DNA are shown in Figure 4c. As it is observed, all cathodic peak currents (i_{pc}) of DIN vary linearly with the $\upsilon^{1/2}$, rather than the υ. These results indicate that the mass transport of DIN to the HMDE surface is via a diffusion controlled process (Wang, Xu, Zhaoa, & Hu, 2007). The same process in the presence of ct-DNA was obtained which revealed that the main mass transport of the DIN–DNA complex to the HMDE surface is via diffusion process too (Wang et al., 2007). We concluded that no significance difference existed between diffusion coefficient of DIN and DIN–DNA complex. Our earlier study shows that at pH = 7.3 the viscosity of solution or the blockage of the electrode surface by ct-DNA adsorption does not have any effects on the efficiency of HMDE (Ahmadi et al., 2014), therefore, the decrease in current of DIN could be attributed to the interaction to ct-DNA and produced a non-

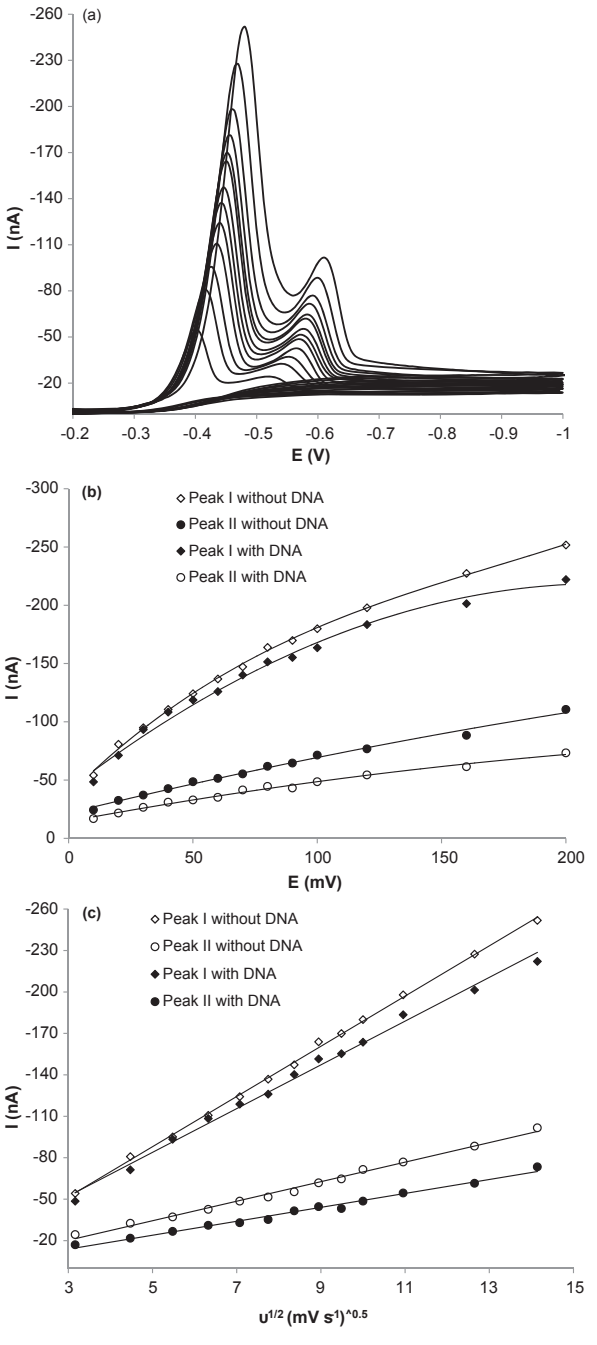

Figure 4. (a) Cyclic voltammograms of 5.0×10^{-5} mol L^{-1} of DIN in absence of ct-DNA in Tris-HCl buffer (0.01 mol L^{-1}, pH 7.3) at various scan rates (10, 20, 30, 40, 50, 60, 70, 80, 90, 10, 120, 160, and 200 mV s^{-1}); (b) The cathodic peak currents (i_{pc}) variation of peaks I, II of DIN (5.0×10^{-5} mol L^{-1}) with scan rate in absence and presence of ct-DNA (5.0×10^{-5} mol L^{-1}); (c) the cathodic peak currents (i_{pc}) variation of peaks I, II of DIN (5.0×10^{-5} mol L^{-1}) with square root of the scan rate in absence and presence of ct-DNA (5.0×10^{-5} mol L^{-1}).

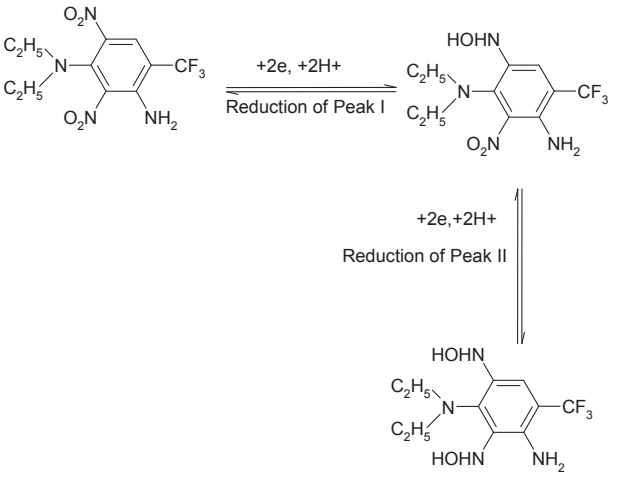

Figure 5. The mechanism of reduction of 5.0×10^{-5} mol L^{-1} of DIN at HMDE in Tris-HCl buffer (0.01 mol L^{-1}, pH 7.3).

electroactive DIN–DNA complex (Ahmadi & Jafari, 2011). However, according to all above data the following mechanism may be proposed for each peak (Figure 5).

The same mechanism for nitro-substituted aromatic compounds, such as nitrobenzene, 2- 3-,4-nitrophenol and 2,4-dinitrophenol, was reported by Ni, Wanga, and Kokot (2001).

3.6. DPV titration of DIN with ct-DNA

The DPV behavior of DIN in the absence and presence of ct-DNA at HMDE is shown in Figure 6a. The voltammogram of DIN without ct-DNA (round dot line) shows two well defined cathodic peaks in the potential of −0.66 to −0.71 V versus Ag/AgCl electrode. By the addition of ct-DNA into 5.0×10^{-5} mol L^{-1} of DIN (r_i = [DNA]/[DIN] = 0.0, 0.1, 0.3, 0.5, 0.7, and 1.0) both cathodic peak potentials were shifted to more negative potentials (25 mV) and i_{pc} was dropped by 75.4%. This substantial diminution of both peak currents is due to formation of slowly diffusing DIN–DNA complex and decrease of free DIN concentration. As it is observed by addition of ct-DNA the formal potential of peaks was shifted to positive potential which is due to the grooves and hydrogen binding interactions (Ahmadi & Ghanbari, 2014). Based upon the decrease in both cathodic peak currents of DIN by addition of ct-DNA, the equilibrium binding constant of DIN–DNA was calculated for peak I (−0.66 V) according to Equation (6) (Ahmadi, Alizadeh, et al., 2011):

$$\frac{1}{[DNA]} = \frac{K(1-A)}{1-\left(\frac{i}{i_0}\right)} - K \tag{6}$$

Where i_0 and i are the cathodic peak currents of DIN in absence and presence of ct-DNA, K is the equilibrium binding constant, and A is the proportionality constant. The plot of 1/[DNA] versus $1/(1-i/i_0)$ yielded a straight line which the equilibrium binding

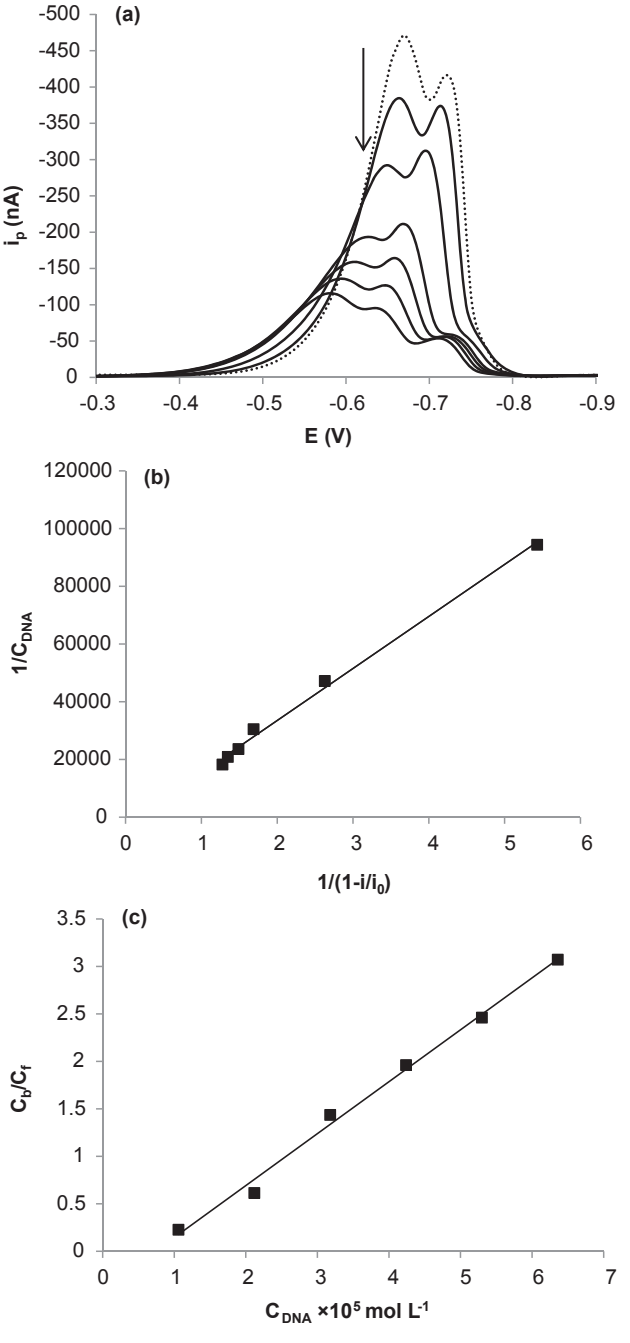

Figure 6. (a) Differential pulse voltammograms of 5×10^{-5} mol L^{-1} of DIN in presence of different amounts ct-DNA (r_i = [DNA]/[DIN] = 0.0, 0.1, 0.3, 0.5, 0.7, 0.8, and 1.0) in Tris–HCl buffer; (b) plot of 1/[DNA] versus $1/1 - i/i_0$ (DIN = 5×10^{-5} mol L^{-1}, scan rate = 70 mV s^{-1}); (c) plot of C_b/C_f versus [DNA] for the determination of binding site size.

constant can be calculated from the intercept (Figure 6b). The results were shown in Table 1.

For calculation of binding site size in terms of base pairs (s) the Equation (7) was used (Aslanoglu & Oge, 2005):

$$\frac{C_b}{C_f} = K\left(\frac{(free\ base\ pairs)}{s}\right) \tag{7}$$

Where C_f and C_b are the concentration of free DIN and DIN–DNA complex, respectively. The concentration of free base pairs in terms of [NP], can be expressed as [DNA]/2. So Equation (7) can be written as:

$$\frac{C_b}{C_f} = K\left(\frac{[DNA]}{2s}\right) \tag{8}$$

The C_b/C_f ratio was determined by the equation (9) as follows (Aslanoglu & Oge, 2005):

$$\frac{C_b}{C_f} = \frac{i_0 - i}{i} \tag{9}$$

By insertion of each K values that calculated according to Equation (6) the mean binding site size can be obtained from the plot of C_b/C_f versus [DNA] (Figure 6c, the data presented in Table 2).

3.6. CV titrations

The CV titration was used for quantifying several interaction parameters of DIN with ct-DNA. By adding ct-DNA to the voltammetric cell containing 5.0×10^{-5} mol L^{-1} of DIN, both cathodic peak currents of DIN decreased and at $R_i = 10$ they were stable (S3).

The values of K_b, binding sit size (s), diffusion coefficients of free (D_f), and bound (D_b) per molecule were measured for only cathodic peak (I) by a nonlinear regression analysis of the experimental data (i_{pc} versus $[R_i]$) than by using of Equation (10).

$$i_{pc} = B\left\{(\alpha n)_f^{\frac{1}{2}} D_f^{\frac{1}{2}} C_t + \left[(\alpha n)_b^{\frac{1}{2}} D_b^{\frac{1}{2}} - (\alpha n)_f^{\frac{1}{2}} D_f^{\frac{1}{2}}\right] \times \left[\frac{b - \left(b^2 - \frac{2K_b^2 C_t^2 R}{s}\right)^{\frac{1}{2}}}{2K}\right]\right\}$$

Table 2. The equilibrium binding constant, binding site size(s), diffusion coefficients of free (D_f), and bounded (D_b) of DIN–DNA complex which obtained by CV and DPV methods.

	Peak I	
Measurement parameters	CV	DPV
$K_{b(298\ K)}$	2.12×10^4	1.98×10^4
$S_{(298\ K)}$	1.05	0.78
$D_{f(cm^2\ s^{-1})}$	7.8×10^{-3}	nm
$D_{b(cm^2\ s^{-1})}$	8.1×10^{-4}	nm

nm, not measured.

$$i_{pc} = B\left\{(\alpha n)_f^{\frac{1}{2}} D_f^{\frac{1}{2}} C_t + \left[(\alpha n)_b^{\frac{1}{2}} D_b^{\frac{1}{2}} - (\alpha n)_f^{\frac{1}{2}} D_f^{\frac{1}{2}}\right] \times \left[\frac{b - \left(b^2 - \frac{2K_b^2 C_t^2 R}{s}\right)^{\frac{1}{2}}}{2K_b}\right]\right\} \quad (10)$$

Where $b = 1 + K_b C_t + \frac{K_b R C_t}{2s}$ and C_t is the total concentration of DIN. In fact, B represents the appropriate, concentration-independent terms in the voltammetric expression and is calculated by Equation (11).

$$B = 2.99 \times 10^5 n A \nu^{\frac{1}{2}} \quad (11)$$

Where, A is area of electrode surface, ν is linear scan rate (mV s^{-1}). In our previous studies, we completely proved Equation (10) and explained all parameters of Equations (10) and (11) (Ahmadi & Jafari, 2011; Ahmadi & Jamali, 2012; Ahmadi, Alizadeh, et al., 2011; Ahmadi, Saberkari, et al., 2013, 2014). The nonlinear fit data are presented in Table 2.

4. Conclusion

In this study, the electrochemical behavior of DIN was studied by CV and DPV. The binding interaction of DIN with ct-DNA was studied by CV, DPV, viscosity titration, competitive fluorescence, UV-Vis, and FT-IR spectroscopy. The combination of spectroscopic and voltammetric techniques are helpful for understanding the mechanism of action of pesticides with target biomolecules and may be useful to design safer pesticides with fewer side effects. The binding of DIN with ct-DNA caused a significance changes in electrochemical and spectral characteristics of DIN, while a little change was observed in ct-DNA solution. The binding constant and the thermodynamic parameters of DIN–DNA complex were also reported. The values of $\Delta H_{bin.}$, $\Delta S_{bin.}$, and ΔG_{bin} (T = 290.65 K) of the DIN–DNA complex were +39.25 kJ mol^{-1}, +215.71 J mol^{-1} and −23.45 KJ mol^{-1}, respectively. These data revealed that the endothermic binding has its origin in the hydrophobic interactions. Also the high positive ΔS_{bin} was explained according to the DIN structure that optimized by mechanical quantum calculations. These data confirmed that the interaction mode of DIN with ct-DNA is major groove with binding site size of 1.

Acknowledgments

We gratefully acknowledge Vice Chancellor for Research and Technology, Kermanshah University of Medical Sciences for financial support. This study was part of a research proposal with No. 91001 in the Novel Drug Delivery Research Center, Faculty of Pharmacy, Kermanshah University of Medical Sciences, Kermanshah, Iran.

Disclosure statement

No potential conflict of interest was reported by the authors.

Supplemental data

Supplemental data for this article can be accessed xxxx.

References

Ahmadi, F., Alizadeh, A. A., Bakhshandeh-Saraskanrood, F., Jafari, B., & Khodadadian, M. (2010). Experimental and computational approach to the rational monitoring of hydrogen-bonding interaction of 2-imidazolidinethione with DNA and guanine. *Food and Chemical Toxicology*, *48*, 29–36.

Ahmadi, F., Alizadeh, A. A., Shahabadi, N., & Rahimi-Nasrabadi, M. (2011). Study binding of Al–curcumin complex to ds-DNA, monitoring by multispectroscopic and voltammetric techniques. *Spectrochimica Acta Part A*, *79*, 1466–1474. doi:10.1016/j.saa.2011.05.002

Ahmadi, F., & Bakhshandeh, F. (2009). In vitro study of damaging effects of 2,4-dichlorophenoxyacetic acid on DNA structure by spectroscopic and voltammetric techniques. *DNA and Cell Biology*, *28*, 527–533.

Ahmadi, F., Ebrahimi-Dishabi, N., Mansouri, K., & Salimi, F. (2014). Molecular aspect on the interaction of zinc-ofloxacin complex with deoxyribonucleic acid, proposed model for binding and cytotoxicity evaluation. *Research in Pharmaceutical Sciences*, *9*, 367–383.

Ahmadi, F., & Ghanbari, K. (2014). Proposed model for binding of permethrin and deltamethrin insecticides with ct-DNA, a structural comparative study. *Ecotoxicology and Environmental Safety*, *106*, 136–145.

Ahmadi, F., & Jafari, B. (2011). Voltammetry and spectroscopy study of in vitro interaction of fenitrothion with DNA. *Electroanalysis*, *23*, 675–682.

Ahmadi, F., Jafari, B., Rahimi-Nasrabadi, M., Ghasemi, S., & Ghanbari, K. (2013). Proposed model for in vitro interaction between fenitrothion and DNA, by using competitive fluorescence, 31P NMR, 1H NMR, FT-IR, CD and molecular modeling. *Toxicology in Vitro*, *27*, 641–650.

Ahmadi, F., & Jamali, N. (2012). Study of DNA-deltamethrin binding by voltammetry, competitive fluorescence, thermal denaturation, circular dichroism, and atomic force microscopy techniques. *DNA and Cell Biology*, *31*, 811–819.

Ahmadi, F., Jamali, N., Jahangard-Yekta, S., Jafari, B., Nouri, S., Najafi, F., & Rahimi-Nasrabadi, M. (2011). The experimental and theoretical QM/MM study of interaction of chloridazon herbicide with ds-DNA. *Spectrochimica Acta Part A*, *79*, 1004–1012.

Ahmadi, F., Jamali, N., Moradian, R., & Astinchap. B. (2012). Binding studies of pyriproxyfen to DNA by multispectroscopic atomic force microscopy and molecular modeling methods. *DNA and Cell Biology*, *31*, 259–268.

Ahmadi, F., Saberkari, M., Abiri, R., & Mohammadi Motlagh, H. (2013). In vitro evaluation of Zn–norfloxacin complex as a potent cytotoxic and antibacterial agent, proposed model for DNA binding. *Applied Biochemistry and Biotechnology*, *170*, 988–1009.

Aslanoglu, M., & Oge, N. (2005). Voltammetric, UV absorption and viscometric studies of the interaction of norepinephrine with DNA. *Turkish Journal of Chemistry*, *29*, 477–485.

Bard, A. J., & Faulkner, L. R. (2004). *Elecrochemical methods fundamentals and applications* (2nd ed.). New York, NY: Wiley.

Becke, A. D. (1993). Density-functional thermochemistry. III. The role of exact exchange. *The Journal of Chemical Physics*, *98*, 5648.

Berg, G. L. (1974). *Farm chemicals handbook* (1st ed.). Willoughby, ON: Meister.

Colominas, C., Luque, F. J., & Teixido, J. (1999). Cavitation contribution to the free energy of solvation. Comparison of different formalisms in the context of MST calculations. *Chemical Physics*, *240*, 253–264.

El-Gogary, T. M., & Koehler, G. (2007). Interaction of psoralens with DNA-bases (I). An ab initio quantum chemical, density functional theory and second-order Møller–Plesset perturbational study. *Journal of Molecular Biology*, *808*, 97–109.

El-Khadem, M., Zahran, M., & El-Kazzaz, M. K. (1979). Effect of the herbicides trifluralin, dinitramine and fluometuron on rhizoctonia disease in cotton. *Plant and Soil*, *51*, 463–470. doi:10.1007/BF02277568

Frisch, M. J., Trucks, G. W., Schlegel, H. B., Scuseria, G. E., Robb, M. A., Cheeseman, J. R., … Gonzalez, C. J. A. (2003). *Pople, Gaussian 03, Inc*. (pp. 239–335). Pittsburgh, PA: Gaussian Inc.

Frost, G., Brown, T., & Harding, A.-H. (2011). Mortality and cancer incidence among British agricultural pesticide users. *Occupational Medicine*, *61*, 303–310.

Hans, C., Becker, B., & Am, J. (1997). DNA binding properties of 2,7-diazapyrene and its N-methylated cations studied by linear and circular dichroism spectroscopy and calorimetry. *Chemical Society Reviews*, *119*, 5798–5803.

Kashanian, S., Askari, S., Ahmadi, F., Omidfar, K., Ghobadi, S., & AbasiTarighat, F. (2008). In vitro study of DNA interaction with clodinafop-propargyl herbicide. *DNA and Cell Biology*, *27*, 581–586.

Kashanian, S., Gholivand, M. B., Ahmadi, F., & Ravan, H. (2008). Interaction of diazinon with DNA and the protective role of selenium in DNA damage. *DNA and Cell Biology*, *27*, 325–332.

Ling, X., Zhong, W., Huang, Q., & Ni, K. J. (2003). Spectroscopic studies on the interaction of pazufloxacin with calf thymus DNA. *Journal of Photochemistry and Photobiology B: Biology*, *93*, 172–178.

Liu, L. (2012). Progress of the mechanism on cancer induced by pesticides. *Advanced Materials Research*, *518–523*, 3179–3182.

Miehlich, B. A., Savin, H. S., & Preuss, H. (1989). Results obtained with the correlation energy density functionals of Becke and Lee, Yang and Parr. *Chemical Physics Letters*, *157*, 200–206.

Miertus, S., Scrocco, E., & Tomasi, J. (1981). Electrostatic interaction of a solute with a continuum a direct utilization of ab initio molecular potentials for the prevision of solvent effects. *Chemical Physics*, *55*, 117–129.

Ni, Y., Wanga, L., & Kokot, S. (2001). Simultaneous determination of nitrobenzene and nitro-substituted phenols by differential pulse voltammetry and chemometrics. *Analytica Chimica Acta*, *431*, 101–113.

N'soukpoe-Kossi, C. N., Ahmed Ouameur, A., Thomas, T., Shirahata, A., Thomas, T. J., & Tajmir-Riahi, H. A. (2008). DNA interaction with antitumor polyamine analogues: Comparison with biogenic polyamines, *Biomacromolecules*, *9*, 2712–2718.

Olson, L. E., Allen, J. L., Mauck, W. L., & Agric, J. (1975). Dinitramine: Residues in and toxicity to freshwater fish. *Food Chemistry*, *23*, 437–439.

Petersson, G. A., & Al-Laham, M. A. (1991). A complete basis set model chemistry. II. Open-shell systems and the total energies of the first-row atoms. *The Journal of Chemical Physics*, *94*, 6081.

Roux, B., & Simonson, T. (1999). Implicit solvent models. *Biophysical Chemistry*, *78*, 1–20.

Sathiakumar, N., MacLennan, P. A., Mandel, J., & Delzell. E. (2011). A review of pidemiologic studies of triazine herbicides and cancer. *Critical Reviews in Toxicology*, *41*, 1–34.

Smith, R. A., Belle, W. S., Shen, K. W., & Woods, W. G. (1973). The degradation of dinitramine (N3,N3-diethyl 2,4-dinitro-6-trifluoromethyl-m-phenylenediamine) in soil. *Pesticide Biochemistry and Physiology*, *3*, 278–288.

Stoytcheva, M. (2011). *Pesticides, the impacts of pesticides exposure* (1st ed.). Croatia: InTech.

Thompson, C. Z., Hill, L. E., Epp, J. K., & Probst, G. S. (1983). Nitrobenzene and 2, 4-and 2, 6-dinitroaniline have also been examined for U0S induction in the liver. *Environmental and Molecular Mutagenesis*, *5*, 803–811.

Wang, F., Xu, Y., Zhaoa, J., & Hu, S. (2007). Electrochemical oxidation of morin and interaction with DNA. *Bioelectrochemistry*, *70*, 356–362. doi:10.1016/j.bioelechem.2006.05.003

Waring, M. J. (1965). Complex formation between ethidium bromide and nucleic acids. *Journal of Molecular Biology*, *13*, 269–282.

Wilson, W. D., Barton, H. J., Tanious, F. A., Kong, S. B., & Strekowski, L. (1990). The interaction with DNA of unfused aromatic systems containing terminal piperazino substituents. *Biophysical Chemistry*, *35*, 227–243.

Zhang, G., Hu, X., Zhao, N., Li, W., & He, L. (2010). Studies on the interaction of aminocarb with calf thymus DNA by spectroscopic methods. *Pesticide Biochemistry and Physiology*, *98*, 206–212.